

2025

Study of the Relationship for Neutron and Proton Skin Thickness on the Neutron Equation of State for ^{18}Ne - ^{180}O Pair Mirror Nuclei

Sala Sami Hamza

Department of Physics, College of Science for Women, University of Baghdad, Baghdad, Iraq,
sala.s@csu.uobaghdad.edu.iq

Ban Sabah Hameed

Department of Physics, College of Science for Women, University of Baghdad, Baghdad, Iraq,
bansh_phy@csu.uobaghdad.edu.iq

Follow this and additional works at: <https://bsj.researchcommons.org/home>

How to Cite this Article

Hamza, Sala Sami and Hameed, Ban Sabah (2025) "Study of the Relationship for Neutron and Proton Skin Thickness on the Neutron Equation of State for ^{18}Ne - ^{180}O Pair Mirror Nuclei," *Baghdad Science Journal*: Vol. 22: Iss. 1, Article 18.

DOI: 10.21123/bsj.2024.10512

Available at: <https://bsj.researchcommons.org/home/vol22/iss1/18>

This Article is brought to you for free and open access by Baghdad Science Journal. It has been accepted for inclusion in Baghdad Science Journal by an authorized editor of Baghdad Science Journal.



RESEARCH ARTICLE

Study of the Relationship for Neutron and Proton Skin Thickness on the Neutron Equation of State for ^{18}Ne - ^{18}O Pair Mirror Nuclei

Sala Sami Hamza^{ID}, Ban Sabah Hameed^{ID} *

Department of Physics, College of Science for Women, University of Baghdad, Baghdad, Iraq

ABSTRACT

Within the framework of the shell model, the single-particle wave functions of Hartree-Fock approximation adopted with Skyrme interactions like Skxtb, Skxs25, Sly4 and Bsk9 to get the thickness of the neutron skin, the mirror radii and the charges mirror radii for ^{18}Ne - ^{18}O pair mirror nucleus. The wave functions were calculated using the NuShellX@MSU shell model code. The computed values of root-mean-square-radii are influenced by the type of interaction employed. The symmetry energy and its slope at nuclear saturation density and the mirror energy displacement were also determined. Comparisons between theoretical and experimental data were made and it was concluded that the data are well described in of this pair mirror nucleus

Keywords: Mirror energy displacement, Occupancies, Pair mirror nuclei, Slope parameter, Symmetry energy

Introduction

The determination of the charge radius is a critical aspect of non-standard atomic nuclei, and throughout the past few years, experts in nuclear physics have focused their efforts on measuring and calculating this quantity. Investigating the charge radius is particularly fascinating as it entails using electromagnetic interaction probes to determine the electric charge of a nucleus. This approach effectively mitigates the considerable uncertainties associated with nuclear physics arising from the strong interaction.^{1–6}

The shell model and some other models provide a brief overview of the properties of atomic nuclei, focusing on essential factors related to nuclear matter, such as volume energy, equilibrium density, incompressibility, symmetry energy (E_{sym}), and symmetry energy slope (L). These quantities are commonly employed to characterize and make comparisons among nuclear models.⁷ The determination

of the isovector parameters E_{sym} and L is challenging due to the limited availability of isotopic chains with relatively small lengths. The isovector indications that show the most potential factors of interamongst are neutron radii, neutron skins, dipole polarizability, and parity-violating asymmetry. These signs have been extensively studied and documented in references. In recent literature, it has been proposed that the disparity in charge radii between mirror nuclei, denoted as $\Delta R_{\text{mirr}}^{\text{ch}}$, can potentially function as an isovector indication for estimating the E_{sym} parameter L .⁷

The nuclear equation of state (NEOS) for infinite nuclear matter, albeit a simplified model, serves as a valuable tool for studying nuclear interactions inside the medium. The distinguishing factor between pure neutron matter and asymmetric nuclear matter is the degree of neutron excess. Neutrons do not exhibit a bound state within a nucleus, hence an excess of neutrons within a nucleus results in a reduction of the binding energy. This

Received 26 December 2023; revised 23 February 2024; accepted 25 February 2024.
Available online 1 January 2025

* Corresponding author.

E-mail addresses: sala.s@csw.uobaghdad.edu.iq (S. S. Hamza), bansh_phy@csw.uobaghdad.edu.iq (B. S. Hameed).

<https://doi.org/10.21123/bsj.2024.10512>

2411-7986/© 2025 The Author(s). Published by College of Science for Women, University of Baghdad. This is an open-access article distributed under the terms of the Creative Commons Attribution 4.0 International License, which permits unrestricted use, distribution, and reproduction in any medium, provided the original work is properly cited.

phenomenon, while required, is inherently unstable and contributes to the manifestation of symmetry energy.⁸

A comprehensive understanding of energy of nuclear symmetry can offer valuable insights into various physical processes related to different profiles of densities and energy levels. The comprehension of nuclear structure is significantly dependent on the nuclear shell model. Furthermore, the behavior of nuclear symmetry energy.⁹ Recent research has shown that the L parameter and the R_{skin} in neutron rich nuclei in to be proportional to the variations in the R_{ch}^{mirr} of mirror nuclei. Neutron skin in atomic nuclei influences the size of neutron stars, the equation of state of nucleonic matter, and the structure of neutron-rich nuclei. Accurately measuring the R_{skin} of nuclei is challenging, despite its importance as a fundamental characteristic. The R_{skin} of the nucleus is determined by the disparity in charge radii between mirror nuclei, which is influenced by the charge symmetry of nuclear forces. Precise calculation of the R_{skin} necessitates the exact assessment of the root-mean-square -radii (rms) of the charge and the neutron skin.¹⁰

The ΔR_{ch} was computed using the radii of charge of the $^{36,38}\text{Ca}$ nuclei for the mirror pairs $^{36}\text{Ca}/\text{S}$ and $^{38}\text{Ca}/\text{Ar}$, which were established by Brown *et al.*¹¹ They determined that the L parameter at the density of nuclear saturation, together with the accompanying R_{ch} , is fixed at a value of 5–70 MeV. This decision excludes a substantial number of predictive models about an equation of state.

Naito *et al.*¹² studied the effect of isospin symmetry breaking (ISB) on the variation in charge radius between mirror nuclei ^{48}Ca and Ni . It was shown that nuclear isospin symmetry-breaking (ISB) effects might potentially modify the anticipated value of the symmetry energy slope parameter L by over 10 MeV. However, the influence of Coulomb corrections could be disregarded.

This study utilized the Hartree-Fock approximation (HF) of the shell model to calculate various properties such as matter, proton, and neutron densities, root mean square (rms) matter and charge radii, occupancy numbers, the variation in the proton radii of the mirror nuclei (R_{mirr}), thickness of neutron skin (R_{skin}), and radii of mirror charges (R_{ch}^{mirr}) which are proportional to NEOS equations at saturation density. Furthermore, the symmetry energy (E_{sym}) and its slope (L), and the displacement energy of the mirror (MDE) were computed for the mirror and subsequently compared with the existing data. The objective of these computations was to ascertain the composition of ^{18}Ne - ^{18}O , and analyze the structure of these mirriors nuclei pair.

Theoretical formalism

The ground density distribution $\rho_{0,t_z}(r)$ at the final state $|\alpha\rangle$ and the initial state $|\beta\rangle$ with ($J_i = J_f$ and $J = 0$), as given by,¹³

$$\rho_{0,t_z}(r) = \frac{1}{\sqrt{4\pi}} \frac{1}{\sqrt{2J_i + 1}} \sum_{\alpha\beta} OBDM(J_i, J_f, 0, \alpha, \beta) \times \langle j_\alpha \| Y_0 \| j_\beta \rangle R_{n_{\alpha l_\beta}}(r) R_{n_{\alpha l_\beta}}(r) \quad (1)$$

Where, $\langle j_\alpha \| Y_0 \| j_\beta \rangle = (-1)^{2j+1} \sqrt{\frac{2j+1}{4\pi}}$, and $OBDM(J_i, J_f, 0, \alpha, \beta)$ is the one body density matrix elements that were calculated using the NuShellX@MSU shell model code.¹⁴ The total matter density is given by:

$$\rho_{0,m}(r) = \rho_{0,p}(r) + \rho_{0,n}(r) \quad (2)$$

The average square radius for matter $\langle R^2 \rangle_\lambda$ proton, and neutron is defined as:¹⁵

$$\langle R^2 \rangle_\lambda = \frac{1}{\lambda} \sum occ\# b^2 \left(N + \frac{3}{2} \right) \quad (3)$$

N , is The total number of excited oscillator quanta represented by λ , which corresponds to the mass, proton, and neutron number.

The formula for the mean square charge radius is:¹

$$\langle R_{ch}^2 \rangle = \langle R_p^2 \rangle + 0.769 - \frac{N}{Z} 0.1161 + 0.033 \quad (4)$$

The R_{ch} of a free proton is 0.769; R_p is the radius of a nucleus's point proton dispersion, a free neutron's charge radii are -0.1161 , and the so-called Darwin-Foldy term is 0.033.¹

The radius of proton dispersion within a nucleus characterized by the proton number (Z) and neutron number (N) should correspond to the radius of neutron distribution observed in mirror nuclei with the neutron number (N) and proton number (Z). The thickness of the neutron skin, denoted as $R_{skin}(Z, N)$, can be expected to accurately represent. The disparity in proton radii among mirror-nuclei, denoted as $R_{mirr}(Z, N)$:¹⁶

$$R_{skin}(^AX) \equiv R_n(Z, N) - R_p(Z, N) \approx R_p(N, Z) - R_p(Z, N) \equiv R_{mirr}(Z, N) \quad (5)$$

The root-mean-square-radius (rms) of protons and neutrons is denoted by R_n and R_p , respectively. The difference in ΔR_{ch} of rms for charge radii R_{ch} of the mirror nuclei is given by:^{16,17}

$$\Delta R_{ch} = R_{ch}(Z, N) - R_{ch}(N, Z) \quad (6)$$

The symmetry energy at the density of nuclear matter saturation ($\rho_0 = 0.16$ nucleons/fm³) is

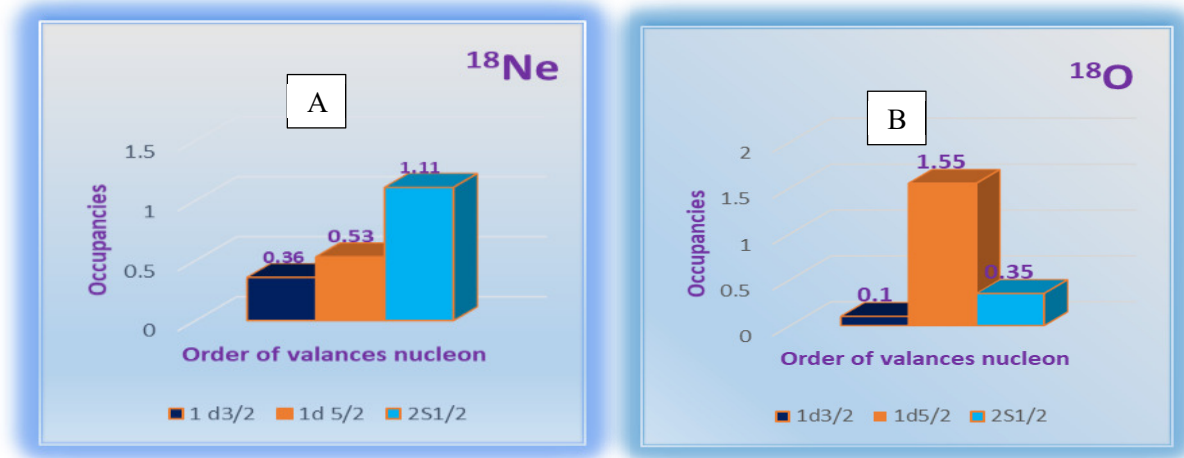


Fig. 1. The occupancies for the ground states of ¹⁸Ne-¹⁸O pair mirror nuclei.

provided by:¹⁸

$$E_{\text{sym}}(\rho) \approx 31.6 \left(\frac{\rho}{\rho^0} \right)^\gamma \quad (7)$$

where $\gamma = 0.69 - 1.05$. The slope symmetry energy is provided by and proportional to the neutron skins and is provided by:⁸

$$L = 3\rho \left[\frac{\partial E_{\text{sym}}(\rho)}{\partial \rho} \right]_{\rho=\rho^0} \quad (8)$$

The parameter L plays a critical role in the application of the NEOS method to both low and high densities, this is crucial for comprehending the structure characteristics of mirror nuclei. When taking into account the Coulomb interaction, one might expect the energy disparity between two mirror nuclei. This energy difference is a clear manifestation of the electromagnetic interaction that is responsible for the phenomena of isospin-symmetry-breaking. The mirror displacement energy (MDE) is defined based on the difference in binding energies (BE) of mirror nuclei. The equation for the mean directional error (MDE) can be expressed as the difference between the backscatter echoes (BE) obtained at temperature T with a vertical beam pointing downward ($T_z = -T$) and the backscatter echoes obtained at temperature T with a vertical beam pointing upward¹⁹ ($T_z = +T$).

$$\text{MDE} = \text{BE}(T, T_z = -T) - \text{BE}(T, T_z = +T) \quad (9)$$

Results and discussion

In this paper, some properties of ¹⁸Ne-¹⁸O mirror nuclei are calculated using large-scale shell model

simulations using the single-particle wave functions of Hartree-Fock approximation (HF) adopted with Skyrme interactions used to produce single-body potentials using Skxtb,²⁰ Skxs25,²¹ Sly4,²² and Bsk9²³ parameterizations. The parameters in the Hartree-Fock approximation are a suitable representation of the Skyrme power. At present, the optimal framework is exemplified by self-consistent mean field models.²⁴ The Skyrme interaction represents the one that is most commonly used in nuclear structure computations that depend on momentum because of its zero-range interaction, which greatly simplifies computations in many-body systems.²⁴

When calculating the occupancies of the nucleus, the primary features of mirror nuclei can be represented. Stated differently, the nucleon's contribution and distribution throughout each state determines the nuclear quantities.¹ Pair mirror ¹⁸Ne-¹⁸O nuclei consist of a central core of ¹⁶O and two nucleons that surround the core and travel in $1d_{3/2}$, $1d_{5/2}$, and $2s_{1/2}$ orbits. The inert core is arranged in configurations ($1s_{1/2}$),⁴ ($1p_{3/2}$),⁸ and ($1p_{1/2}$).⁴ The average quantity of nucleons within every j-level located beyond the core is displayed in Fig. 1. (A&B). It's obvious for ¹⁸Ne that The greatest ratio of proton is in the $2s_{1/2}$ orbit but for ¹⁸O the dominant orbit of neutrons at $1d_{5/2}$. The lower percentage configuration mixture appeared for $1d_{3/2}$ orbit with 36% and 1% for ¹⁸Ne and ¹⁸O, respectively. In general, the inclusion of $2s_{1/2}$ and $1d_{5/2}$ has a powerful effect in obtaining interesting results. This is due to a clear high percentage configuration mixture of these states.

To examine the variations in the ground state characteristics of the mirror nuclei, the matter density distributions $\rho_m(r)$, $\rho_p(r)$ and $\rho_n(r)$ of the pair mirror using the four Skyrme interactions (Skxtb, Skxs25, Sly4,

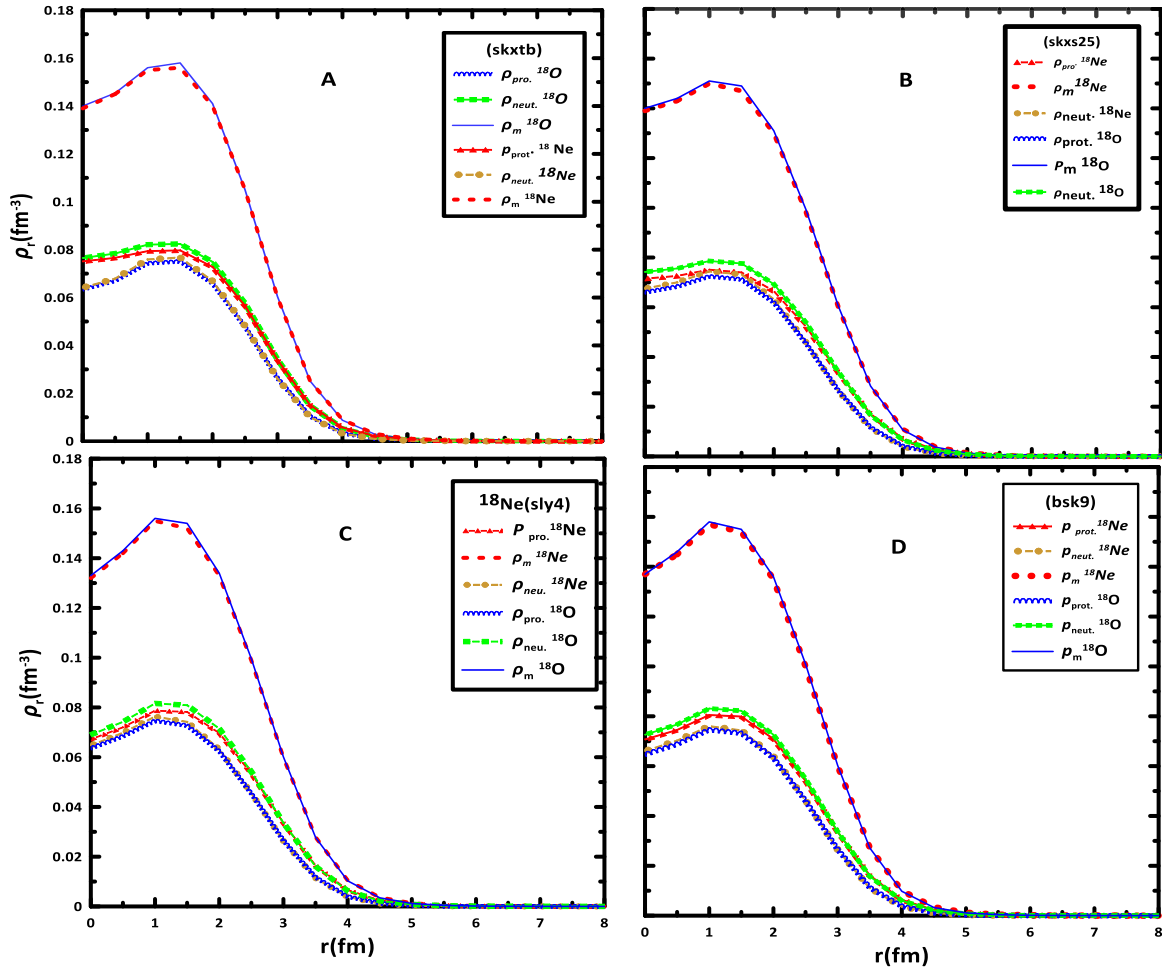


Fig. 2. The matter density distributions $\rho_m(r)$, $\rho_p(r)$ and $\rho_n(r)$ of ^{18}Ne - ^{18}O pair mirror nuclei.

and Bsk9) are displayed in Fig. 2. (A- D), respectively. The curves in this figure represent the predicted matter, proton and neutron densities of the nuclei and their mirror counterparts, determined using the many-body interaction. It is noticeable from the figure that the computed density distribution for all interactions closely aligns with each other, at $r \geq 2$ fm. By comparing the current results with the results of other research,²⁵ the same shape was obtained for the density values, but with different amounts. This difference is due to the diversity of the interactions used, which leads to different wave functions.

One of the few observable static characteristics of atomic nuclei is their nuclear radii, which include the proton (R_p), neutron (R_n), matter (R_m), and charge (R_{ch}) radii. These radii can depict the important aspects of the nuclear structure. These calculated root mean square radii (rms) with different Skyrme interactions and available measured values^{26,27} of the R_m and R_{ch} of pair mirror nuclei are shown in Table 1. For the results, the values of R_{ch} and R_m agree with the

experimental data for all Skyrme interactions except when using Skxs25 interaction is slightly greater than the experimental results.

When calculating the nuclear radii values for mirror nuclei, the result of the spatial transformation effect of protons and neutrons with the HF eigen functions appears because only the diagonal matrix components of the single particle eigen function, which contributes to the nuclear radii, are present in the nuclear radii calculations.

Proton-rich atomic nuclei have a proton-to-neutrons ratio that is noticeably greater than that of stable nuclei. Because there are more neutrons than protons in the neutron-rich nucleus, it is known as such and has a neutron skin.²⁸ The disparity between the nuclei that are abundant in protons and those that are abundant in neutrons in the present investigation was demonstrated by the calculations R_{skin} of the utilized nuclei. The asymmetry in the neutron occurs due to the shift in the proton density relative to neutrons as a result of the Coulomb interaction. A

Table 1. Determine the rms values for the radii of protons, neutrons, matter, and charge for ^{18}Ne - ^{18}O using four Skyrme interactions. The computed R_{ch} & R_m are compared with the predicted data.^{26,27}

Nucleus	Interaction	rms (fm)			
		R_p	R_n	R_{ch}	R_m
^{18}Ne	Skxtb	2.856	2.645	2.938	2.764
	Skxs25	2.969	2.710	3.049	2.857
	Sly4	2.914	2.699	2.995	2.820
	Bsk9	2.880	2.686	2.962	2.796
	Exp.	–	–	2.9714 ± 0.0076 ²⁶	2.81 ± 0.14 ²⁷
^{18}O	Skxtb	2.666	2.802	2.729	2.743
	Skxs25	2.739	2.894	2.800	2.826
	Sly4	2.717	2.863	2.780	2.799
	Bsk9	2.702	2.836	2.764	2.777
	Exp.	–	–	2.7726 ± 0.0056 ²⁶	2.61 ± 0.08 ²⁷

Table 2. Determine the radii of the mirror, skin, and mirror charges. ^{18}Ne - ^{18}O using four Skyrme interactions. The computed R_{ch}^{mirr} are in comparison to the empirical data.²⁶

Interaction	R_{ch}^{mirr}	R_{mirr}	R_{skin} for ^{18}Ne	R_{skin} for ^{18}O	R_{ch}^{mirr} Exp.
Skxtb	0.209	0.19	–0.210	0.136	0.1988 ± 0.002 ²⁶
Skxs25	0.249	0.23	–0.260	0.155	
Sly4	0.215	0.197	–0.215	0.145	
Bsk9	0.198	0.178	–0.194	0.134	

higher neutron-to-proton ratio, or neutron skin, is a characteristic of the neutron-rich nucleus.²⁹ The phenomenon occurs when there is an overabundance of neutrons in the nucleus's core region, which causes a pressure differential. A portion of the excess neutrons are driven toward the outer regions of the nucleus by this pressure differential.

Despite having little effect on the nucleus's overall size, the neutron skin provides important insights into the dynamics of nucleon interactions in a substantially isospin-asymmetric environment, particularly concerning density variations.²⁸ It also presents the R_{skin} of the mirror partners and the disparity in proton radii for the mirror pair R_{mirr} . Indeed, the R_{skin} of the mirror nuclei that have an excess of neutrons is less than the proton skins when comparing similar levels of asymmetry between protons and neutrons. When there is an excess of protons ($Z - N$), it has been observed that the thickness of the proton skin is greater than the thickness of the neutron skin corresponds to the neutron excess ($N - Z$) in a nucleus. The cause of this phenomenon is attributed to the Coulomb repulsion between protons.³⁰

For present results, the R_{skin} of the mirror nuclei ^{18}Ne - ^{18}O are calculated using four sets of HF potentials shown in Table 2. The negative values of R_{skin} for ^{18}Ne because this nucleus is a proton-rich, the skin is called proton skin, where the calculated results were in agreement with each other except Bsk9 set. As for the ^{18}O nucleus, different values were obtained for

R_{skin} , neutron skin, due to the different reactions used. One can conclude the variations in the masses' kinetic energy operators of the protons and neutrons cause a slight variance in the pair mirror's R_{skin} findings, which changes depending on the type of interaction performed. The computed value of R_{ch}^{mirr} when using the Bsk9 set wave function is 0.198 fm. Approximates the experimental value 0.1988 ± 0.002 .²⁶ It was found that the imbalance in the neutron shell results from the Coulomb interaction, which boosts the proton density outward relative to the neutrons.

The relation between the R_m radii and the mass number (A) and between the ΔR_{ch} and ΔR_{skin} are very essential to studying the differences between the pair of mirror nuclei. The calculations indicate that the different Skyrme interactions give nearly linear dependence between R_m and the mass number as shown in Fig. 3. The values R_m for ^{18}O nucleus when using Skxs25 (green color) and SLy4 (red color) sets for Skyrme interactions are agreement with the experimental data²⁷ (black color), but the values of R_m for ^{18}Ne nucleus are greater than the experimental data for each set of Skyrme interactions. The reason for this is due to the acquired values of proton skins. Fig. 4 represents the relationship between ΔR_{ch} and ΔR_{skin} using different Skyrme interactions. The relationship between them is a linear, decreasing relationship. The investigation of proton radii in mirror nuclei is valuable due to the challenging nature of experimental measurements of neutron distributions. The proton radius can serve as a substitute for measuring the R_{skin} . Additionally, the neutron radius is graphed with the proton radius of the mirror nucleus. The linear correlation between ΔR_{ch} and ΔR_{skin} can be utilized to approximate the neutron radii of rare isotopes that have not yet been empirically accessible.

The nuclear matter's E_{sym} at saturation density, as well as its complete reliance on density, has received significant focus in the last few years. The E_{sym} quantifies the alteration in the system's binding

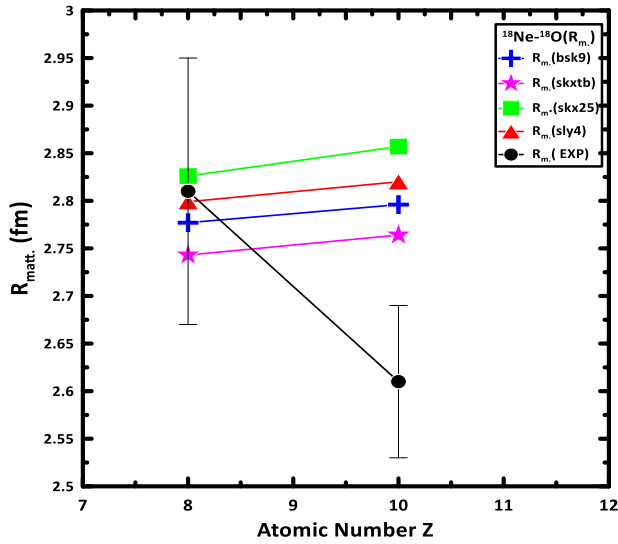


Fig. 3. The relationship between R_m radii and the mass number using different Skyrme interactions. The experimental data are taken for Ref.²⁷

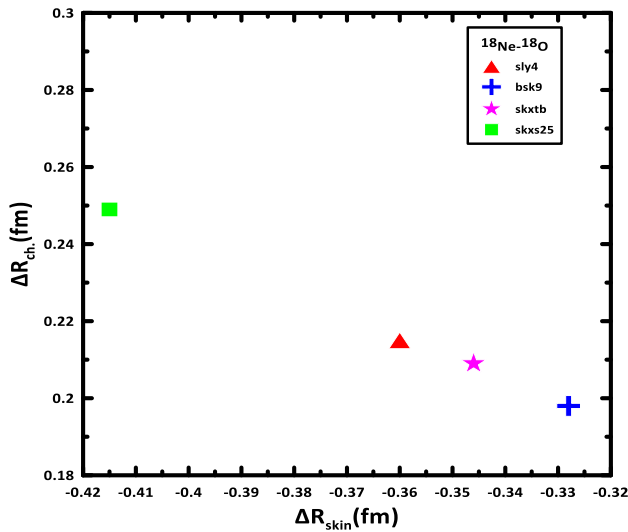


Fig. 4. The relationship between ΔR_{ch} and ΔR_{skin} using different Skyrme interactions.

as the ratio of neutrons to protons varies while keeping the whole number of particles constant. Consequently, it can be conceptualized as the relationship between symmetry energy and density. It has been demonstrated that nuclear models with small E_{sym} values can lead to instability.

Comprehending the density dependence of nuclear E_{sym} is essential to comprehend the structure of nuclei. The relationship between the density and symmetry energy (E_{sym}) in the Hartree-Fock (HF) approximation, with four Skyrme interactions Skxtb, Skxs25, Sly4, and Bsk9 parameterizations are shown in Fig. 5. An empirical observation reveals a nearly

Table 3. The computed values of L parameter and MED for ^{18}Ne - ^{18}O mirror nuclei.

Mirror Nuclei	Interaction	(L) (MeV)		MED (MeV)	
^{18}Ne - ^{18}O	skxtb	Cal.	Exp. ³¹	Cal.	Exp. ³³
	Skxs25	99.05	106 ± 37	7.938	7.663
	Sly4	98.85		7.966	
	Bsk9	99.30		7	
		99.06		7.086	

linear correlation between the E_{sym} and the ratio of nuclear matter density to its saturation density.

In order to ascertain the properties of nuclear matter, one can investigate the nuclear equation of state by calculating the values of slope parameter L using different Skyrme set interactions. The calculated L of ^{18}Ne - ^{18}O pair mirror nuclei is in the range $98.85 \leq L \leq 99.3 \text{ MeV}$, which are in agree with the measured value $106 \pm 37 \text{ MeV}$,³¹ which are shown in Table 3. The results for L , however, demonstrate a significant agreement with further estimates published in the literature, particularly for energy density functional. The relationship between the difference in charge radii, ΔR_{ch} , for mirror pairs and the quantities $|N - Z| \times L$ may be demonstrated. The difference in neutron skin ΔR_{skin} exists by the product of the absolute difference between the number of neutrons and protons $|N - Z|$ and the slope parameter L , together with a component that is mostly unaffected by the magnitude of the difference between neutrons and protons $|N - Z|$.³² The L term becomes dominant when the absolute difference between N and Z is high. However, when the absolute difference between N and Z approaches zero, only the E_{sym} term remains.⁸ If the charge radii can be determined with a precision of approximately 0.007 fm, the limitation on L derived from the mirror charge radii is superior to that obtained from the anticipated parity-violating electron scattering tests.⁸ Fig. 6, represent the relationship between the difference in charge radius ΔR_{ch} and the slope parameter L . The current results of ΔR_{ch} and L of the mirror nuclei agreement with the experimental data³³ within error after using the potential for Bsk9.

Fig. 7 represent the relationship between the different in neutron skin ΔR_{skin} and the slope parameter L . Different results were obtained between ΔR_{skin} and L with different types of interactions used. Harith and Hameed³³ examined this dependency using HF approximation with SkXs25 parameters, where good results were obtained for the pairs mirror nuclei ^{13}O - ^{13}B and ^{13}N - ^{13}C . In mirror nuclei, the mirror displacement energy (MDE) is the point at which the effects of isospin-symmetry-breaking are most clearly observed. The estimated minimum

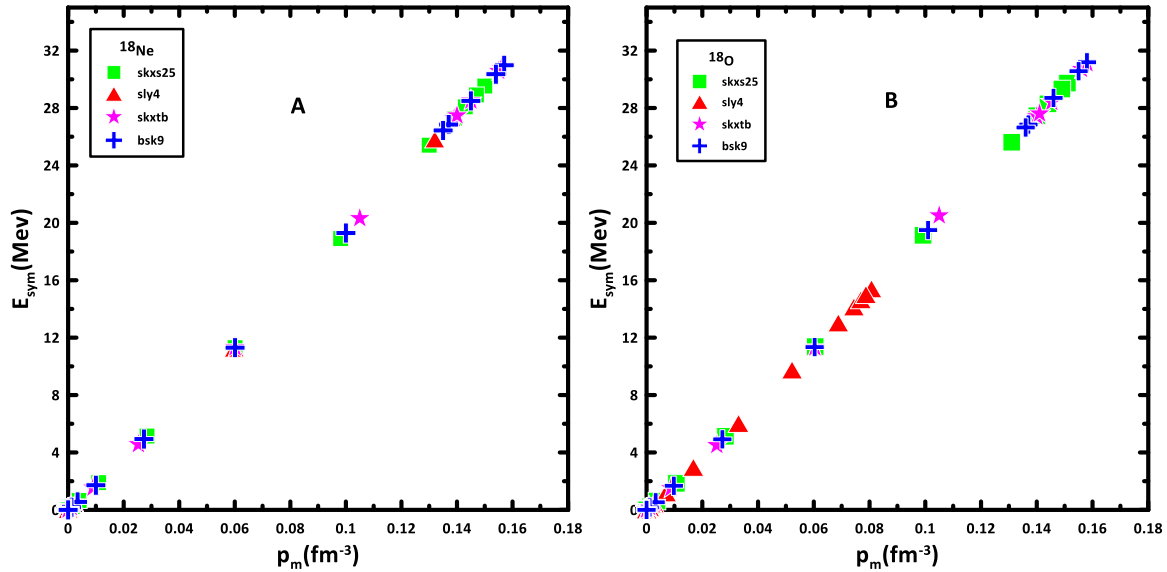


Fig. 5. The connection between the two entities ρ_m & E_{sym} for ^{18}Ne – ^{18}O mirror nuclei.

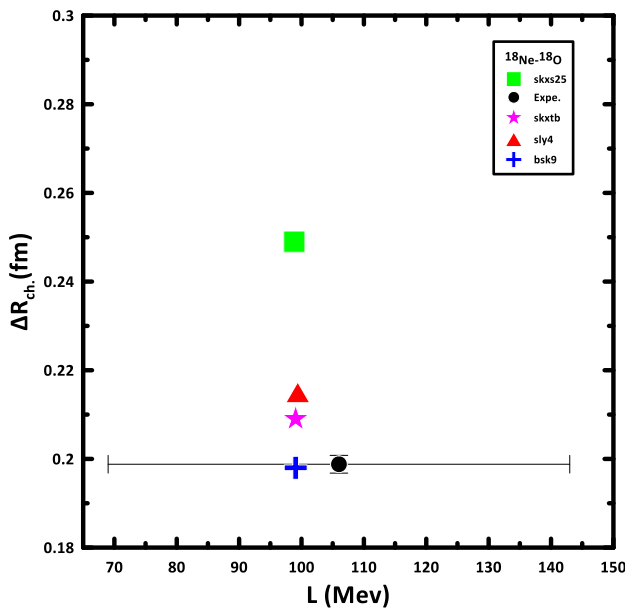


Fig. 6. The relationship between ΔR_{ch} radii and L parameter using different Skyrme interactions.

energy difference (MED) for the ^{18}Ne – ^{18}O mirror nuclei, using the Skxtb, Skxs25, Sly4, and Bsk9 interactions, slightly deviate from the observed value of 7.663 MeV³⁴. These values are displayed in Table 3.

Conclusion

This paper investigated the nuclear structure of a mirror nucleus with mass number 18 utilizing four Skyrme interactions. The most significant contribution to the current examination of the ^{18}Ne

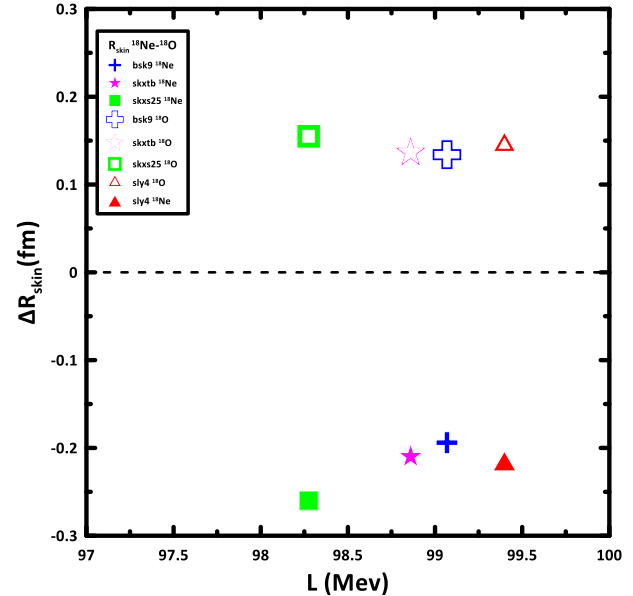


Fig. 7. The relationship between ΔR_{skin} radii and L parameter using different Skyrme interactions.

nucleus showed a considerable contribution that the main orbit of a proton is in the $2s_{1/2}$, while the highest ratio of neutrons for ^{18}O is at $1d_{5/2}$. This is caused by these states' very high proportion configuration mixture.

The matter density distributions $\rho_m(r)$, $\rho_p(r)$ and $\rho_n(r)$ of the pair mirror for all interactions tightly align at $r \geq 2$ fm and diverge at r less than 2 fm regions. This discrepancy results from the variety of interactions that are employed, which produces various wave functions.

The values of R_{ch} and R_m agree with the experimental data for Skyrme interactions except when using Skxs25 interaction. This results from the difference in the kinetic energy operator between the masses of protons and neutrons. When utilizing the Bsk9 set wave function, the computed value of R_{ch}^{mirr} approaches the experimental value. This is because it was discovered that the Coulomb contact, which causes the protons' density to be pushed outward about the neutrons, is what causes the imbalance in the neutron shell. There is a linear relationship between the E_{sym} and the computed density of nuclear matter. The computations of the MDE were agreed based on the information currently available regarding the various binding energies of the mirror nuclei. The restriction on L values determined from the mirror charge radii comes from ^{18}Ne - ^{18}O pair mirror nuclei with $98.85 \leq L \leq 99.3$ MeV, which agrees with the observed value.

Author's declaration

- Conflicts of Interest: None.
- We hereby confirm that all the Figures and Tables in the manuscript are ours. Furthermore, any Figures and images, that are not ours, have been included with the necessary permission for republication, which is attached to the manuscript.
- No animal studies are present in the manuscript.
- No human studies are present in the manuscript.
- Ethical Clearance: The project was approved by the local ethical committee at University of Baghdad.

Authors' contributions statement

S S H and B S H both contributed to visualizing and designing the study, obtaining data, in addition to analyzing and interpreting the results, and writing the manuscript.

References

1. Hameed BS, Alwan TA. Study the Nuclear Structure of Some Even-Even Ca Isotopes Using the Microscopic Theory. *Baghdad Sci J.* 2023;20(1):235–244.(10). <https://dx.doi.org/10.21123/bsj.2022.6924>.
2. Guan D, Pei J, Jiang C. Implications on Skyrme equations of state from neutron skin measurements. *Chin. Phys. C.* 2024;48(6):0641055. <https://doi.org/10.48048/tis.2022.4169>.
3. Hameed BS, Rejah BK. Study the Nuclear Structure of Some Cobalt Isotopes. *Baghdad Sci J.* 2022;19(6):1566. <https://dx.doi.org/10.21123/bsj.2022>.
4. Hussein AAM, Flaiyh GN. Theoretical Study of Matter Density Distributions, and Elastic Electron Scattering Form Factors of Exotic Nuclei (^{26}F and ^9C). *East Eur J Phys.* 2023(1):82–88. <https://doi.org/10.26565/2312-4334-2023-1-09>.
5. Raheem SK, Dakhil ZA, Hameed BS. Effect of the Exact Center of Mass Correction on the Longitudinal Form Factors for Neutron Rich $^{12,14,18}\text{N}$ Isotopes. *J. Phys.: Conf. Ser.* 2021;1829(1):012023. <https://doi.org/10.1088/1742-6596/1829/1/012023>.
6. Coraggio L, De Gregorio G, Gargano A, Itaco N, Fukui T, Ma YZ, *et al.* Shell-model study of calcium isotopes toward their dripline. *Phys Rev C.* 2020;102(5):054326.(9). <https://doi.org/10.1103/PhysRevC.102.054326>.
7. Reinhard PG, Nazarewicz W. Information content of the differences in the charge radii of mirror nuclei. *Phys Rev C.* 2022;105(2):7. <https://dx.doi.org/10.1103/PhysRevC.105.L021301>.
8. Pineda SV. Constraints on the Neutron Equation of State Using the Difference in 54 Ni-54 Fe Mirror Pair Charge Radii: Michigan State University. Phd thesis. 2022;24.
9. An R, Sun S, Cao L-G, Zhang F-S. Constraining the nuclear symmetry energy with charge radii of the mirror pairs nuclei. *Nucl Sci Tech.* 2023;34:119. <https://doi.org/10.1007/s41365-023-01269-1>.
10. Mohammed RA, Majeed WZ. Exotic Structure of ^{17}Ne - ^{17}N and ^{23}Al - ^{23}Ne Mirror Nuclei. *East Eur J Phys.* 2022;4:72–9.8. <https://doi.org/10.26565/2312-4334-2022-4-05>.
11. Brown BA, Minamisono K, Piekarewicz J, Hergert H, Garand D, Klose A, *et al.* Implications of the ^{36}Ca - ^{36}S and ^{38}Ca - ^{38}Ar difference in mirror charge radii on the neutron matter equation of state. *Phys Rev Res.* 2020;2:022035(R). <https://doi.org/10.1103/PhysRevResearch.2.022035>.
12. Naito T, Roca-Maza X, Colo G, Liang H, Sagawa H. Isospin symmetry breaking in the charge radius difference of mirror nuclei. *Phys Rev C.* 2022;106:L061306. <https://doi.org/10.1103/PhysRevC.106.L061306>.
13. Brown BA, Radhi R, Wildenthal BH. Electric quadrupole and hexadecupole nuclear excitations from the perspective of electron scattering and modern shell-model theory. *Phys Rep.* 1983;101(5):313. [https://doi.org/10.1016/0370-1573\(83\)90001-7](https://doi.org/10.1016/0370-1573(83)90001-7).
14. Brown BA, Rae W. The shell-model code NuShellX@ MSU. *Nucl Data Sheets.* 2014;120:115–118. <https://doi.org/10.1016/j.nds.2014.07.022>.
15. Abdulhasan AA, Dakhil ZA. Electric quadrupole transition in neutron rich $^{32-42}\text{S}$ -isotopes with different model. *Int J Nonlinear Anal Appl.* 2022;13:3127–3137. <https://doi.org/10.22075/IJNAA.2022.6783>.
16. Yao Xua J, Zheng Li Z, Hua Suna B, Fei Niu Y, Roca- Mazac X, Sagawad H, *et al.* Constraining equation of state of nuclear matter by charge-changing cross section measurements of mirror nuclei. *Phys Lett B.* 2022;833:137333. <https://doi.org/10.1016/j.physletb.2022.137333>.
17. Kumar P, Bishakha NT, Thakur V, Kumar R, Dhiman SK, editors. A study of trends of neutron skin thickness and proton radii of mirror nuclei. *Proceedings of the DAE Symp. On Nucl Phys.* 2022;2:300–301.
18. Chen L-W, Ko CM, Li B-A. Determination of the stiffness of the nuclear symmetry energy from isospin diffusion. *Phys Rev Lett.* 2005;94:032701. <https://doi.org/10.1103/PhysRevLett.94.032701>.
19. Bentley MA. Excited States in Isobaric Multiplets-Experimental Advances and the Shell-Model Approach. *Physics.* 2022;4(3):995–1011. <https://doi.org/10.3390/physics4030066>.
20. Brown B, Duguet T, Otsuka T, Abe D, Suzuki T. Tensor interaction contributions to single-particle energies. *Phys Rev C.* 2006;74(6):061303. <https://doi.org/10.1103/PhysRevC.74.061303>.

21. Brown BA, Shen G, Hillhouse G, Meng J, Trzcińska A. Neutron skin deduced from antiprotonic atom data. *Phys. Rev C*. 2007;76(3):034305. <https://doi.org/10.1103/PhysRevC.76.034305>.
22. Chabanat E, Bonche P, Haensel P, Meyer J, Schaeffer R. A Skyrme parametrization from subnuclear to neutron star densities Part II. Nuclei far from stabilities. *Nucl Phys A*. 1998;635(1–2):231–56. [https://doi.org/10.1016/S0375-9474\(98\)00180-8](https://doi.org/10.1016/S0375-9474(98)00180-8).
23. Goriely S, Samyn M, Pearson J, Onsi M. Further explorations of Skyrme–Hartree–Fock–Bogoliubov mass formulas.IV: Neutron-matter constraint. *Nucl Phys A*. 2005;750(2–4):425–43. <https://doi.org/10.1016/j.nuclphysa.2005.01.009>.
24. Geng J, Xiang J, Sun BY, Long WH. Relativistic Hartree-Fock model for axially deformed nuclei. *Phys Rev C*. 2020;101(6):064302. <https://doi.org/10.1103/PhysRevC.101.064302>.
25. Ma H-L, Dong B-G, Yan Y-L, Zhang H-Q, Zhang X-Z. Proton Pygmy Dipole Resonances in $^{17,18}\text{Ne}$: Collective non collective excitations. *Phys Rev C*. 2012;85:044307. <https://doi.org/10.1103/PhysRevC.85.044307>.
26. Angeli I, Marinova KP. Table of experimental nuclear ground state charge radii: An update. *At Data Nucl Data Tables*. 2013;99(1):69–95. <https://doi.org/10.1016/j.adt.2011.12.006>.
27. Ozawa A, Baumann T, Chulkov L, Cortina D, Datta U, Fernandez J, *et al*. Measurements of the interaction cross sections for ArandCl isotopes. *Nucl Phys A*. 2002;709 (1–4):60–72. [https://doi.org/10.1016/S0375-9474\(02\)01071-0](https://doi.org/10.1016/S0375-9474(02)01071-0).
28. Punta P, Lay JA, Moro AM. Transfer reactions of exotic nuclei including core deformations: ^{11}Be and ^{17}C . *Phys Rev C*. 2023;108:024613. <https://doi.org/10.1103/PhysRevC.108.024613>.
29. Hussein AAM, Flaiyh GN. Theoretical Study of Proton Halo Structure and Elastic Electron Scattering Form Factor for ^{23}Al and ^{27}P Nuclei by Using Full Correlation Functions (Tensor Force and Short Range). *East Eur J Phys*. 2023;1:75–8. <https://doi.org/10.26565/2312-4334-2023-1-08>.
30. Gaidarov M, Moumene I, Antonov A, Kadrev D, Sarriuren P, de Guerra EM. Proton and neutron skins and symmetry energy of mirror nuclei. *Nucl Phys A*. 2020;1004:122061. <https://doi.org/10.1016/j.nuclphysa.2020.122061>.
31. Reed BT, Fattoyev FJ, Horowitz CJ, Piekarewicz J. Implications of PREX-2 on the equation of state of neutron-rich matter. *Phys Rev Lett*. 2021;126:1–17:172503. <https://doi.org/10.1103/PhysRevLett.126.172503>.
32. Harith RH, Hameed BS. Study of the Symmetry Energy and the Nuclear Equation of State for ^{13}O , ^{13}B and ^{13}N - ^{13}C Mirror Nuclei. *Iraqi J phys*. 2023;21:24–31. <https://doi.org/10.30723/ijp.v21i4.1147>.
33. Wang M, Huang WJ, Kondev FG, Audi G, Naimi S. The Ame2020 atomic mass evaluation (II). Tables, graphs and references. *Chin Phys C*. 2021;45:030003. <https://doi.org/10.1088/1674-1137/abddaf>.

دراسة العلاقة بين سمك القشرة النيوتروني والبروتوني على معادلة الحالة النيوترونية لزوج النوى المرآتية ^{18}O - ^{18}Ne

سلا سامي حمزه، بان صباح حميد

قسم الفيزياء، كلية العلوم للبنات، جامعة بغداد، بغداد، العراق.

الخلاصة

في إطار نموذج القشرة، تم اعتماد الدوال الموجية أحادية الجسيم لتقريب هاتري - فوك مع تفاعلات سكيرم مثل Skxtb ، Skxs25 ، Sly4 ، و Bsk9 لحساب سمك القشرة النيوتروني، ونصف قطر المرآتي ونصف قطر الشحنة المرآتية، لزوج النوى المرآتية $^{18}\text{Ne-O}$. تم حساب الدوال الموجية باستخدام كود نموذج القشرة NuShellX@MSU . تتأثر القيم المحسوبة لجذر متوسط نصف القطر المربع بنوع التفاعلات المستخدمة. كما تم تحديد طاقة التناظر وانحدارها عند كثافة التشبع النووي وازاحة طاقة النوى المرآتية. تم إجراء مقارنات بين البيانات النظرية والتجريبية وتم التوصل إلى أن البيانات موصوفة بشكل جيد لهذا الزوج من النواة المرآتية.

الكلمات المفتاحية: أزاحة طاقة النوى المرآتية، أعداد الأشغال، زوج النوى المرآتية، معامل الانحدار، طاقة التناظر.